Biological Psychiatry: CNNI

Archival Report

Prediction of Behavioral Improvement Through Resting-State Electroencephalography and Clinical Severity in a Randomized Controlled Trial Testing Bumetanide in Autism Spectrum Disorder

Erika L. Juarez-Martinez, Jan J. Sprengers, Gianina Cristian, Bob Oranje, Dorinde M. van Andel, Arthur-Ervin Avramiea, Sonja Simpraga, Simon J. Houtman, Richard Hardstone, Cathalijn Gerver, Gert Jan van der Wilt, Huibert D. Mansvelder, Marinus J.C. Eijkemans, Klaus Linkenkaer-Hansen, and Hilgo Bruining

ABSTRACT

BACKGROUND: Mechanism-based treatments such as bumetanide are being repurposed for autism spectrum disorder. We recently reported beneficial effects on repetitive behavioral symptoms that might be related to regulating excitation-inhibition (E/I) balance in the brain. Here, we tested the neurophysiological effects of bumetanide and the relationship to clinical outcome variability and investigated the potential for machine learning–based predictions of meaningful clinical improvement.

METHODS: Using modified linear mixed models applied to intention-to-treat population, we analyzed E/I-sensitive electroencephalography (EEG) measures before and after 91 days of treatment in the double-blind, randomized, placebo-controlled Bumetanide in Autism Medication and Biomarker study. Resting-state EEG of 82 subjects out of 92 participants (7–15 years) were available. Alpha frequency band absolute and relative power, central frequency, long-range temporal correlations, and functional E/I ratio treatment effects were related to the Repetitive Behavior Scale-Revised (RBS-R) and the Social Responsiveness Scale 2 as clinical outcomes.

RESULTS: We observed superior bumetanide effects on EEG, reflected in increased absolute and relative alpha power and functional E/I ratio and in decreased central frequency. Associations between EEG and clinical outcome change were restricted to subgroups with medium to high RBS-R improvement. Using machine learning, medium and high RBS-R improvement could be predicted by baseline RBS-R score and EEG measures with 80% and 92% accuracy, respectively.

CONCLUSIONS: Bumetanide exerts neurophysiological effects related to clinical changes in more responsive subsets, in whom prediction of improvement was feasible through EEG and clinical measures.

https://doi.org/10.1016/j.bpsc.2021.08.009

Autism spectrum disorder (ASD) is a heterogeneous group of neurodevelopmental disorders (1), of which some forms require pharmacological intervention to cope with severe social, sensory, and affective symptoms (2). At present, only two antipsychotic drugs are registered to reduce irritability, often at the cost of serious side effects (3). Novel treatments are being developed on the basis of specific pathophysiological mechanisms, which have been indicated in studies with animal models of genetic disorders (4). Some of these new approaches are based on existing drugs, which may facilitate their implementation (5,6). However, drug repurposing is accompanied by extensive variability in treatment responses in conventional ASD trials (7). Successful application may depend on incorporation of functional brain measures related to the hypothesized mechanistic effects (8). Here, we show the results of the first randomized controlled ASD medication trial to incorporate quantitative electroencephalography (EEG) before and after treatment.

A large body of literature exists on quantitative EEG in ASD (9–11), which may inform ASD treatment development. For instance, excitation/inhibition (E/I) ratio dysregulation has become an important pathophysiological target in ASD since both changes in inhibition and excitation have been implicated (12–15). We and others have shown that E/I ratio may be quantified at the network level using EEG (16,17), which may have purpose in understanding treatment effects and clinical responses as indicated by preclinical studies and open-label trials (18–23). To date, no pharmacological placebo-controlled clinical trials have used pre- and post-treatment EEG measurements, a strategy that has been tested for non-pharmacological interventions such as neurofeedback and repetitive transcranial magnetic stimulation (24–26). Following

ISSN: 2451-9022

a similar path as in antidepressant trials (27–29), evaluation of EEG biomarkers in ASD together with machine learning analysis may show promise to develop treatment prediction models.

To test the potential of EEG analysis for treatment optimization for ASD, we developed Bumetanide in Autism Medication and Biomarker (BAMBI) (EudraCT 2014-001560-35), the first completed randomized, placebo-controlled ASD medication trial to incorporate EEG measurements to indicate brain effects of bumetanide and to develop stratification and prediction biomarkers of treatment response. Bumetanide is a diuretic drug currently repurposed for ASD treatment. It acts as a selective chloride importer NKCC1 antagonist, which is important to regulate intraneuronal chloride concentration and GABA (gamma-aminobutyric acid) polarity. Animal models have shown that the postnatal GABA shift through down-regulation of NKCC1 activity is abolished, leading to excitatory actions of GABA and increased network activity (30,31). From these findings, it was postulated that bumetanide may have favorable clinical effects since elevated E/I has become an important theory in autistic development (12–15).

The potential neurologic effect of bumetanide has been disputed, given its poor brain bioavailability due to limited crossing of the blood-brain-barrier (32). Several trials have nonetheless shown promising effects on ASD symptomatology (33–35). We recently published the clinical results of the BAMBI study; although there was no superior effect on the primary Social Responsiveness Scale 2 (SRS-2) end point between placebo and bumetanide, we did find a superior effect of bumetanide on the Repetitive Behavior Scale-Revised (RBS-R), a scale of core symptomatology. In addition, a subgroup of most responsive individuals seemed delineated from that of placebo-treated individuals (36). It is plausible that particularly these subgroups share a mechanistic element targeted by bumetanide. In this subset of participants with stronger improvement, neurophysiological measures may be more prominently related to clinical improvement.

In line with this reasoning, we first hypothesized that resting-state EEG measures would confirm that bumetanide has neurophysiological effects in the brain; second, that clinical improvement would be related to bumetanide's neurophysiological effects; and third, that EEG measures could be used to develop prediction models for bumetanide in ASD. We used a set of alpha frequency band EEG measures that have proven sensitive to the ratio of excitation and inhibition in computational models, including a method to quantify a functional form of E/I at the network level (*f*E/I; see Methods and Materials) (16).

METHODS AND MATERIALS

Study Design and Participants

This study is a secondary analysis of the BAMBI trial (Eudra-CT 2014-001560-35), a single-center, double-blind, participant-randomized, placebo-controlled, phase 2 superiority trial testing bumetanide (twice-daily up to 1.0 mg) in otherwise medication-free children with ASD. The trial included children aged 7–15 years with expert-confirmed ASD diagnosis. Exclusion criteria were an IQ $<$ 55 and use of psychoactive medication. Outcomes were assessed at pretreatment (D0), after 91 days of treatment (D91), and after 28-day washout (D119). Clinical outcome measures were the SRS-2, the RBS-R, and resting-state EEG. The study was approved by the medical ethical committee of the UMC Utrecht, Utrecht, the Netherlands, and all participants or their legal guardians signed informed consent. The CONSORT (Consolidated Standards of Reporting Trials) flow diagram with the included participants and measurements performed is given in Figure 1. Detailed description of the protocol and clinical effects have been published previously (36) and summarized in Supplemental Methods.

EEG Recordings and Preprocessing

EEGs were recorded during 5 minutes of eyes-closed rest with a 64-channel BioSemi system (2048 Hz). EEG analyses were done using the Neurophysiological Biomarker Toolbox and custom-made scripts (37). All recordings were manually cleaned for artifacts and re-referenced to the average reference. After preprocessing, on average 210 seconds per recording (80–327 s) were available for analysis.

EEG Analysis

Computational neuronal network models generating oscillations have shown that changes in excitation and inhibition affect the amplitude, frequency, temporal correlations, and *f*E/I in the alpha band (8–13 Hz) (16,38). Therefore, we applied these measures to the EEG data in the alpha band.

Spectral power was computed using the Welch method with an 8192-point Blackman window and a frequency resolution of 0.125 Hz. Relative alpha power is expressed in percent and was calculated by dividing the absolute power in the alpha band by the integrated power in the range of 1 to 45 Hz. Central frequency provides a measure of the frequency at which most of the power in the alpha band is concentrated. Central frequency has the advantage over peak frequency that it does not require the presence of a strong peak or—as it sometimes appears—that the peak is identified close to 8 Hz because of increasing power at lower frequencies. The detrended fluctuation analysis was used to quantify the long-range temporal correlations in the amplitude fluctuation of alpha oscillations (39). The detrended fluctuation analysis exponents in the interval of 0.5 to 1.0 indicate long-range temporal correlation and rich temporal structure fluctuations, whereas an exponent of 0.5 characterizes an uncorrelated signal. Finally, we used the recently introduced measure of functional E/I ratio (*f*E/I), which has been shown to track pharmacological intervention and reveal large heterogeneity in an ASD sample (16). Inhibition-dominated networks are characterized by an *f*E/I $<$ 1, excitation-dominated networks *f*E/I $>$ 1, and E/I-balanced networks will have *f*E/I = 1. A detailed description of the EEG measures is provided in the Supplement.

Statistical Analysis

The secondary analyses in this paper were conducted according to the predefined statistical analysis in the study protocol, which included the development of EEG biomarkers for stratification and functional assessment of treatment effects [see (36) and trial protocol link in the Supplement].

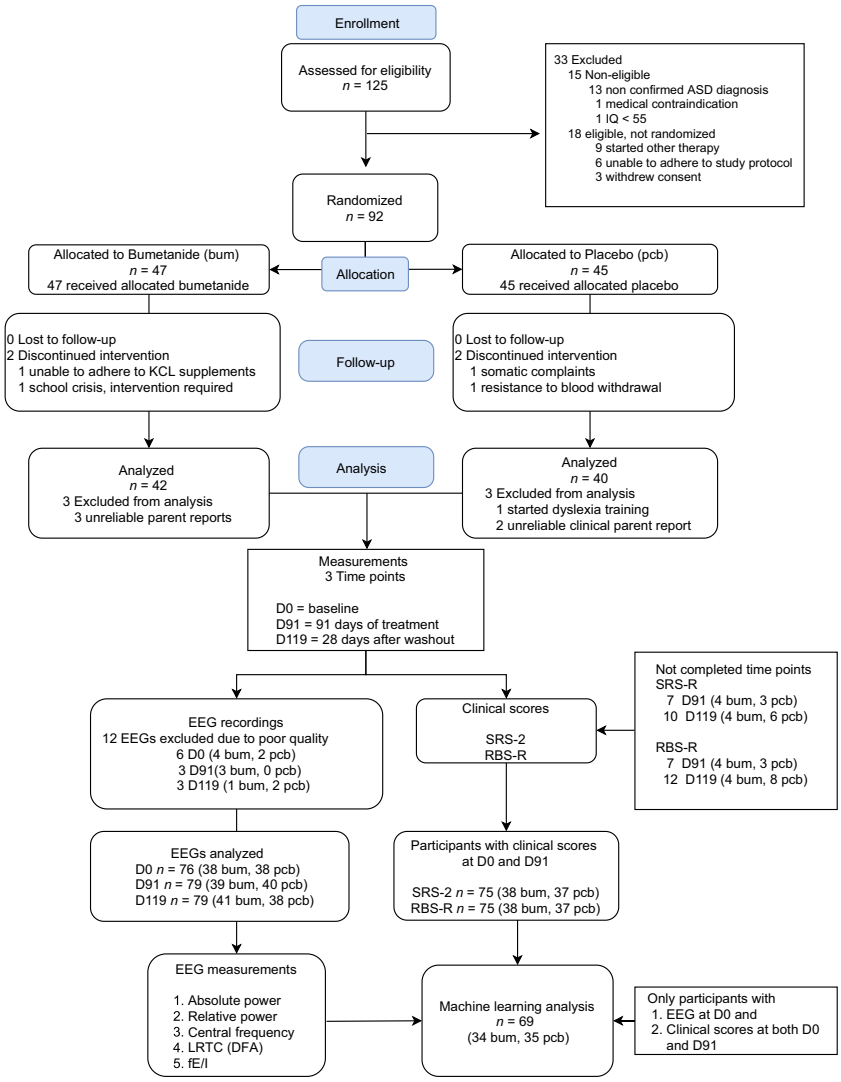

Figure 1. CONSORT (Consolidated Standards of Reporting Trials) flow diagram for the patients included for electroencephalography (EEG) analysis from the Bumetanide in Autism Medication and Biomarker trial. A total of 125 subjects were screened for eligibility between June 2016 to December 2018 at the UMC Utrecht, Utrecht, the Netherlands. Ninety-two participants were randomized to receive bumetanide (n = 47) or placebo (n = 45). EEG recordings of 82 participants were available for analysis (bumetanide n = 42; placebo n = 40). ASD, autism spectrum disorder; DFA, detrended fluctuation analysis; fE/I, functional excitation-inhibition ratio; KCL, potassium chloride; LRTC, long-range temporal correlations; RBS-R, Repetitive Behavior Scale-Revised; SRS-2, Social Responsiveness Scale 2.

Effect of Bumetanide Treatment on EEG Measures

To assess whole-brain treatment effect of bumetanide versus placebo on EEG measures, we analyzed the average biomarker value (mean) of the 64 channels using a linear mixed model (SAS, version 9.4; SAS Institute). Treatment and treatment-by-time interaction were included to assess the difference between bumetanide and placebo and washout effects. Sex, age, and pretreatment EEG measures were included to correct for potential confounding factors (40,41). We derived estimated means for each treatment group and a mean difference between treatment groups at 91 days with 95% confidence intervals and p values. This analysis and the machine learning parts were run as sensitivity analyses, excluding participants with unreliable clinical reports as motivated in the initial report of BAMBI (36). For the EEG effects irrespective of clinical report, we also ran an intention-to-treat analysis. The topographical distribution of EEG treatment effects was analyzed per treatment group by comparing each electrode at different time points using a paired t test. False discovery rate was used to correct for multiple testing at the electrode level (see Supplemental Methods).

Clinical Outcome Analyses

The SRS-2 (primary end point; total raw score; range 0−195; higher score indicates more affected) and RBS-R (secondary end point; total score; range 0−129; higher score indicates more affected) were used to relate EEG parameters to clinical outcome in core symptomatology. The original study findings showed that a subset of participants with the greatest SRS-2 and RBS-R improvement were in the bumetanide group, which we took as a basis to define thresholds for treatment response stratification and prediction. We set a high threshold to indicate the level of clinical improvement outcome above which there were no or few (n = 3 for SRS-2) placebo-treated

subjects present (16 points for RBS-R and 20 points for SRS-2) and may be more successful to identify true responders in terms of effects being related to bumetanide targeting mechanisms. In addition, we defined a medium response threshold, using mean clinical score improvement as a reference (7 and 10 points for RBS-R and SRS-2, respectively) to test stability of stratification and prediction under a medium treatment response threshold. We investigated the association between EEG and symptom change in the whole sample and for the different treatment thresholds to test the stability of correlations under different stratification scenarios.

Machine Learning Models for Clinical Outcome Predictions

The data preprocessing, feature selection, classifier training, and validation steps were performed in RStudio (version 1.3.959) (42) and R (version 4.0) (43). We visualize each step in Figure 2, Figure S1, and Supplemental Methods.

Preprocessing

Features and Improvement Classes. For D91 treatment response predictions from pretreatment EEG using machine learning analysis, we compiled the pool of potential features from 5 resting-state measures on 63 channels. We also incorporated pretreatment SRS-2 and RBS-R scores, total IQ, age, and a binary variable describing whether they had received treatment prior to the study, resulting in a total of 5 clinical features, thus 320 features in total. After data preprocessing, using a shuffle-split technique, which randomly and repeatedly splits the data (44), we created 100 random data partitions for training and 100 random data partitions for out-of-sample validation. In each partition, 80% (±5%) of the data was reserved for training and testing and 20% (±5%) for validation.

Feature selection was performed to identify from the 320 starting features the subsets that could classify subjects for being below or above medium and high response treatment thresholds. This resulted in 100 feature subsets, 1 per training partition. For clinical interpretation of which features were most important in the prediction models, we reported the 10 features with the highest frequency of appearance in 70%-or-higher raw accuracy runs as most informative.

Training, Hyperparameter Tuning, and Testing. A fast implementation of a random forest classifier (45) was trained and optimized 100 times on each of the training sets containing 80% (±5%) of the data, using the feature subsets obtained in the feature selection step using leave-one-out cross-validation.

Validation. The leave-one-out cross-validation results were validated on each of the 100 out-of-sample sets containing 20% (±5%) of the data. The performance measures expressed in terms of balanced and raw accuracy, sensitivity, and specificity were averaged over the out-of-sample runs. We report the raw accuracy showing all the correctly classified observations irrespective of class. Balanced accuracy was reported to even out imbalances between sensitivity and specificity resulting from the higher prevalence of low-clinical-improvement cases (Figure S2).

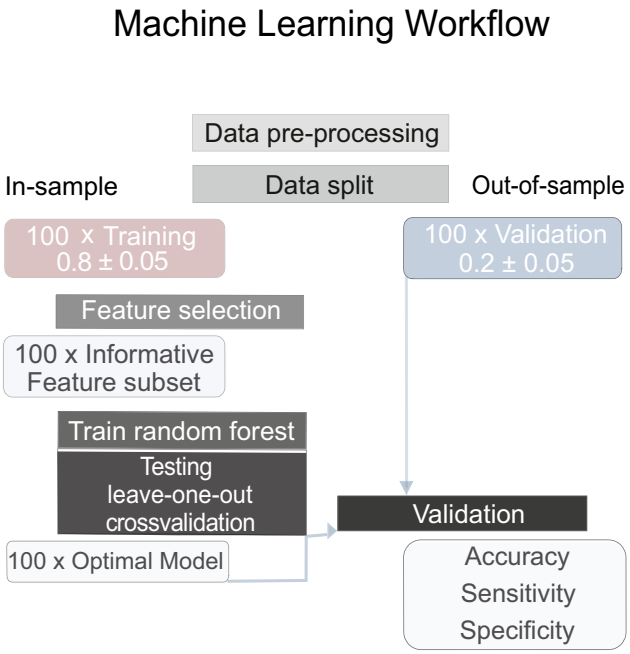

Figure 2. Machine learning workflow. The dataset comprised 5 electroencephalography biomarkers over 63 channels and 5 clinical features used to predict clinical improvement of $n = 34$ bumetanide-treated subjects above or below the thresholds Repetitive Behavior Scale-Revised: 7- and 16-point. To develop and validate the random forests classifier using a shuffle-split method, the data were divided into training and validation sets of 80% and 20%, respectively, with a ±5% margin to ensure a minimum number of above threshold improvement subjects in each validation set. To generalize results and aid replicability, these steps were repeated 100 times, and each time, a new random split was generated. For each of the 100 training splits, the most optimal features were selected using a recursive method to discriminate subjects with outcomes above and below the selected treatment thresholds. The selected feature sets served as input for the random forest classifiers trained on each of the 100 training partitions. This process generated 100 models with different selected feature constellations that were optimized using leave-one-out cross-validation. The resulting optimal models were validated on the out-of-sample partitions. The number of correctly and incorrectly classified datapoints for each of the 100 iterations rendered 100 accuracy results, which were then averaged to obtain overall results for each improvement threshold.

RESULTS

Ninety-two participants were randomized, of whom 88 completed the trial (36). EEG recordings of 82 of these trial completers were available for analysis: 42 from the bumetanide group (mean age 10.5 ± 2.5 years; 14 females) and 40 from the placebo group (mean age 10.5 ± 2.5 years; 12 females). EEG recordings from 10 participants ($n = 12$) were excluded after preprocessing because of poor quality of EEG data or no eyes-closed rest EEG could have been recorded (D0 $n = 6$, D91 $n = 3$, D119 $n = 3$; 1 participant had poor quality EEG at each time point). This left 76 EEGs for analysis at D0, 79 at D91, and 79 at D119 (for details, see Figure 1). Tables S1 and S2 describe the participants included, their demographics,

clinical scores, and EEG biomarker values. To test EEG effects of bumetanide, we investigated 5 EEG measures in the alpha band (8–13 Hz) that have proven sensitive to pharmacological E/I intervention (see Methods and Materials).

Effect of Bumetanide Treatment on EEG Measures

After 91 days, superior EEG effects of bumetanide to placebo were found for absolute power, relative power, *f*E/I, and central frequency (Table 1 and Figure 3A–D). These effects were of medium size (Cohen's $d = 0.5$), except for central frequency showing a small effect size (Cohen's $d = 0.3$). No effects were found between D91 and the D119 washout period. Subanalysis of treatment interaction with age, IQ, and attention-deficit/hyperactivity disorder comorbidity did not show significant effects. These findings were not different in the intention-to-treat analysis (Table S3). Subsequently, we analyzed the topographical distribution of EEG changes between D0 and D91 in each treatment group. Significant effects were only present in the bumetanide group, where absolute power, relative power, and *f*E/I increased and central frequency decreased in a cluster of channels (Figure 3E–H).

Correlation Between EEG Measures and Clinical Outcome

Correlations of EEG biomarker D91-D0 changes with change in SRS-2 or RBS-R after bumetanide treatment did not reveal significant associations at the group level. Stratification by the medium treatment response threshold (RBS-R $\geq$ 7 points improvement [$n = 8$]) did reveal high, significant correlations between an increment in absolute and relative power and RBS-R improvement after bumetanide (Figure 4A, B), albeit just a trend for *f*E/I (Figure 4C). The subgroup with improvement < 7 points ($n = 24$) showed no significant correlations between EEG changes and clinical outcome (Figure 4D, E) or even an opposite trend for *f*E/I by contrast to the $\geq$7 points group (Figure 4C, F). No correlations were found for the RBS-16 threshold or both SRS-2 tested thresholds.

Prediction of Clinical Improvement Through Machine Learning Analysis

To test the potential of clinical outcome predictions, we entered channel-level pretreatment EEG measures together with 5 clinical features (pretreatment SRS-2 and RBS-R scores, total IQ, age, and prior treatment) into a random forest machine learning classifier to predict clinical improvement of bumetanide-treated subjects above or below the thresholds RBS-R: 7- and 16-point, and SRS-2: 10- and 20-point (for details, see Methods and Materials) (Figures 5 and 6; Figure S1). The distributions of the individual change in SRS-2 and RBS-R clinical outcomes in relationship to each of the chosen treatment thresholds are illustrated in Figures 5A and 6A for those individuals included in the machine learning analysis ($n = 34$).

To generalize results and aid replicability, the classifiers were trained in 100 runs using leave-one-out cross-validation and further validated on 100 out-of-sample partitions. For SRS-2, 10- and 20-point improvement predictions, the out-of-sample validation accuracy, sensitivity, and specificity did not exceed chance levels (Figure 5B, C; Figure S3A, B). In contrast, the classifiers predicted 7- and 16-point improvement on RBS-R with 80% and 92% average balanced accuracy, the equivalent of 63% and 86% average sensitivity and 96% and 99% average specificity for each threshold, respectively (Figure 6C; Figure S3C, D). The 16-point RBS-R improvement had a better trade-off between sensitivity and specificity than the 7-point improvement (Figure 6B).

The selection of features with the highest frequency of appearance (out of 100) in runs achieving a high validation accuracy (>70%) revealed that there was no consistent pattern for SRS-2 in the most predictive features (Figure 5D, E), apparently in line with poor prediction success for this scale. RBS-R baseline score was ranked as the most important predictor of RBS-R improvement, followed by EEG features of absolute power and *f*E/I in the parietal and central-parietal regions (Figure 6D, E).

DISCUSSION

The presented analysis of resting-state placebo-controlled EEG measures has implications for the application of bumetanide and potentially for other similar ASD treatments. First, bumetanide and not placebo altered spectral and temporal characteristics of neuronal oscillations, indicating a neurophysiological treatment effect. Second, changes in brain activity after bumetanide were only related to improvement in

Table 1. Superior Effect of Bumetanide to Placebo in Power, Central Frequency, and *f*E/I

	Placebo Group, Mean ± SEM			Bumetanide Group, Mean ± SEM			Treatment Effect	
EEG Biomarker	Baseline, D0, $n = 38$	D91, $n = 38$	D119, $n = 36$	Baseline, D0, $n = 36$	D91, $n = 36$	D119, $n = 36$	Treatment Effect (95% Confidence Interval)	p Value
Absolute Power, μV	10.7 ± 1.2	10.06 ± 1.2	10.1 ± 1.1	8.1 ± 1.1	9.4 ± 1.2	8.4 ± 1	1.44 (0.23 to 2.64)	.02[a]
Relative Power, %	28.5 ± 1.8	29.0 ± 1.9	29.2 ± 1.9	25.5 ± 1.8	27.6 ± 1.9	29.1 ± 1.9	2.4 (0.88 to 4.00)	.0026[a]
Central Frequency, Hz	9.7 ± 0.07	9.8 ± 0.06	9.8 ± 0.07	9.64 ± 0.06	9.6 ± 0.06	9.64 ± 0.05	−0.07 (−0.13 to −0.008)	.03[a]
DFA, β	0.72 ± 0.01	0.73 ± 0.01	0.72 ± 0.02	0.72 ± 0.02	0.71 ± 0.01	0.71 ± 0.02	−0.02 (−0.04 to 0.007)	.2
*f*E/I	1.05 ± 0.02	1.02 ± 0.02	1.03 ± 0.03	1.01 ± 0.02	1.07 ± 0.03	1.04 ± 0.02	0.06 (0.02 to 0.11)	.006[a]

Data are shown for participants who completed D91. Linear mixed model analysis of whole-brain average electroencephalography (EEG) biomarkers reveal superior effect of bumetanide to placebo on absolute power, relative power, central frequency, and *f*E/I after 91 days of treatment. Treatment effect, 95% confidence intervals, and p values are reported.

D0, day 0 baseline recording; D91, day 91 of treatment; D119, day 119 (after 28-day washout period); DFA, detrended fluctuation analysis; *f*E/I, functional excitation-inhibition ratio.

[a]Significance was set at $p < .05$.

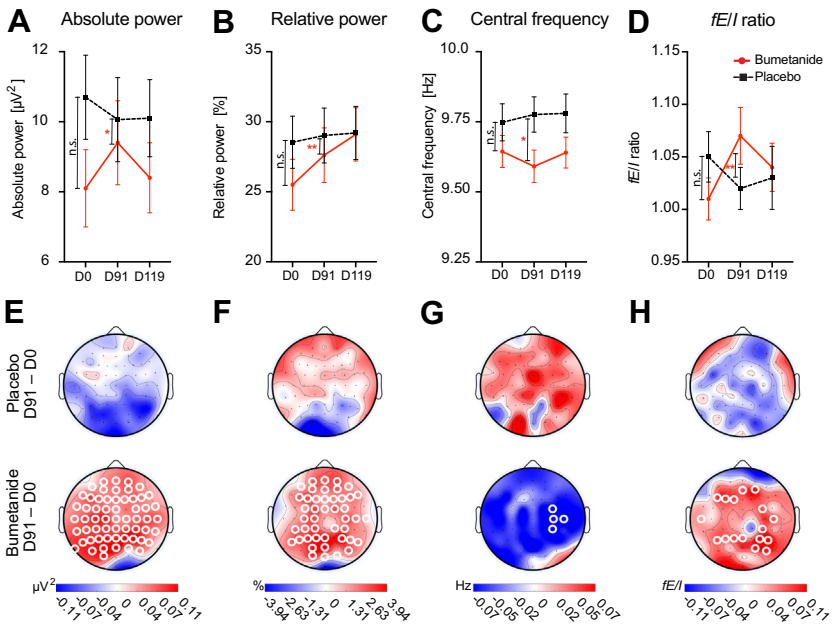

Figure 3. Bumetanide treatment—but not placebo—affects alpha oscillations in children with autism spectrum disorder. **(A–D)** Whole-brain average electroencephalography (EEG) measures at treatment time points. No baseline differences (D0) were found for EEG measures between treatment groups **(A–D)** (*t* test). Linear mixed model analysis of treatment effects (D0–D91) showed a superior effect of bumetanide to placebo in absolute power **(A)**, relative power **(B)**, central frequency **(C)**, and functional excitation-inhibition ratios (*f*E/I) **(D)** (see also Table 1). Analysis of treatment-by-time interaction revealed no washout effect at D119 for any of the EEG measures. Bumetanide group (solid red lines). Placebo group (black dashed lines). Mean ± SEM are plotted. $^{*}p < .05$; $^{**}p < .01$. **(E–H)** Grand-average topographies of the treatment effects on EEG measures (D91−D0). Significant channels are shown in white circles ($p < .05$, false discovery rate corrected) indicating widespread effects in the bumetanide group with an increase in absolute power **(E)**, relative power **(F)**, and *f*E/I **(H)** and a cluster of channels with decreased central frequency **(G)**. No significant channels were found in the placebo group. D0, day 0 baseline recording; D91, day 91 of treatment; D119, day 119 (after 28-day washout period).

repetitive behavior in more responsive subsets. Finally, predictions of improvement in repetitive behavior were feasible by implementing pretreatment EEG and clinical severity in machine learning analysis.

The observed EEG effects suggest that bumetanide enters the brain sufficiently to alter both power and network-level E/I of neuronal oscillations after 91 days of treatment, effects that did not significantly decrease after the washout period. Other studies have indicated functional brain effects of bumetanide in ASD using magnetic resonance spectroscopy and eye tracking, albeit in open-label trial designs (33,46). Previously, EEG effects of bumetanide in ASD and tuberous sclerosis complex have been described in case reports (47,48), and recently, our group also showed bumetanide effects on event-related potentials in a tuberous sclerosis complex open-label study (22). It is possible that brain availability of bumetanide is higher in ASD owing to different pharmacokinetics, a more permeable blood-brain barrier (33), or effects through blood-brain barrier–free areas (e.g., the median eminence) (49,50). Another question is whether the observed EEG effects relate to a shift from depolarizing to hyperpolarizing GABAergic transmission. In healthy subjects, $GABA_A$ receptor positive allosteric

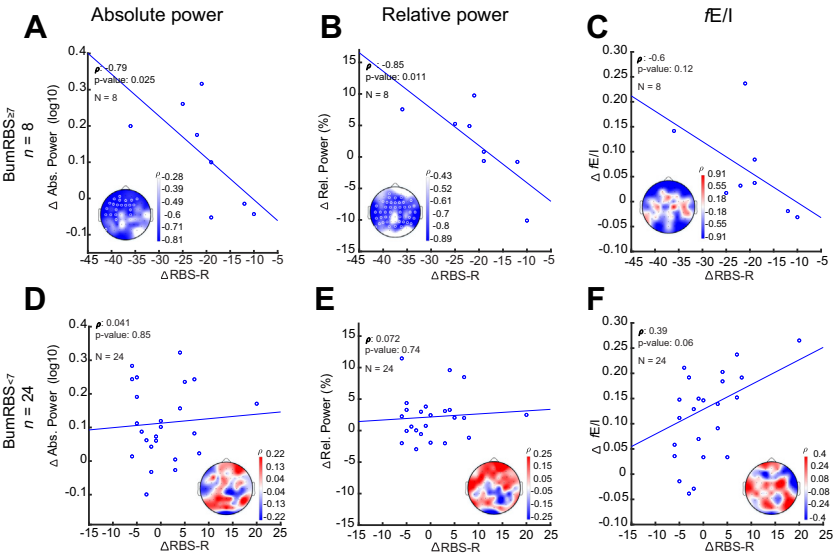

Figure 4. Correlations between electroencephalography and clinical outcome changes in participants with below **(D–F)** and equal to or exceeding **(A–C)** 7 points improvement on the Repetitive Behavior Scale-Revised (RBS-R). **(A, B)** An increment in absolute and relative power after bumetanide was strongly correlated (*rho* ≤ −0.8) to repetitive behavior improvement, in participants with improvement of at least 7 points. **(C)** A medium-high (*rho* = −0.6), albeit nonsignificant, correlation was observed between an increment in functional excitation-inhibition ratio (*f*E/I) and repetitive behavior improvement. **(D, E)** No significant correlations were found between electroencephalography change and repetitive behavior improvement in participants with improvement below 7 points. **(F)** An increase in *f*E/I is moderately (*rho* = 0.4) and borderline significantly ($p = .06$) associated with worsening in repetitive behavior in the opposite direction when compared with the ≥7 points improvement group **(C)**. Correlations were calculated using Spearman correlation coefficient. Channels with significant ($p < .05$, false discovery rate corrected) correlations are shown in white circles. Abs., absolute; Rel., relative.

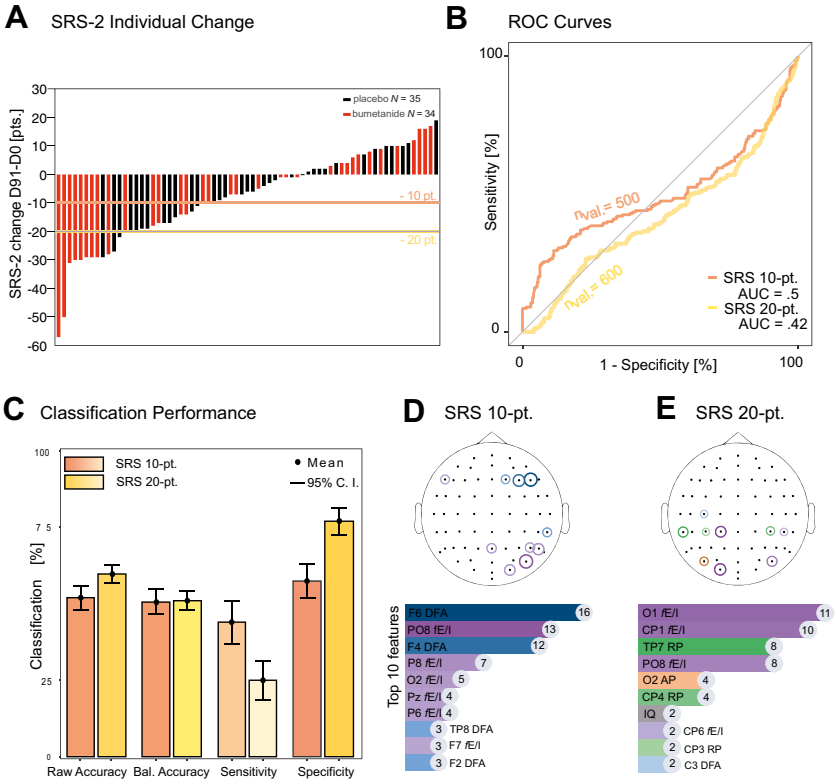

Figure 5. Machine learning delineation between clinical improvement levels did not exceed chance when predicting improvement in social responsiveness. **(A)** Distribution of the individual change in Social Responsiveness Scale 2 (SRS-2) (D91−D0) in relation to treatment thresholds used for machine learning analysis (SRS 10-point orange line and SRS 20-point yellow line). Data presented are only for individuals with pretreatment electroencephalography measures and clinical outcome scores available (bumetanide n = 34, placebo n = 35). **(B)** Receiver operating characteristic (ROC) curves to illustrate the diagnostic ability of the binary classifiers for the different improvement thresholds across the SRS-2 clinical outcome scale. This ability is expressed by the relationship between true (sensitivity) and false-positive rates, as depicted by the ROC curves. The curve for the perfect model that correctly classifies 100% below and above threshold improvers contains the point (0, 1), while a random estimate curve is closer to the nondiscrimination line (gray). An area under the curve (AUC) closer to 1 indicates a classifier having both high sensitivity and specificity. Classifiers for 10- and 20-point SRS improvement demonstrate close to or worse than chance performance. **(C)** Classification performance of SRS 10-point and SRS 20-point treatment thresholds. As per out-of-sample validation, the classifiers predicted 10- and 20-point improvement on SRS-2 with an average sensitivity of 44% and 25% and 57% and 77% average specificity for each threshold, respectively, which corresponded to 56% and 51% average balanced accuracy (mean between specificity and sensitivity), respectively. **(D, E)** The 10 most frequently selected electrodes and electroencephalography measures in iterations exceeding 70% accuracy on out-of-sample validation partitions are shown for the outcome thresholds. Bal., balanced; C. I., confidence interval; D0, day 0 baseline recording; D91, day 91 of treatment; DFA, detrended fluctuation analysis; *f*E/I, functional excitation-inhibition ratio.

modulators such as benzodiazepines have been shown to reduce alpha power (51,52). We recently described a decrease in *f*E/I following the administration of the positive allosteric modulator zolpidem in healthy adults, suggesting enforcement of inhibition, in line with the supposed drug effect (16). Bumetanide seems to show opposite alpha-oscillation effects in terms of power and *f*E/I in ASD when compared with the acute effect of positive allosteric modulators in healthy subjects. A similar opposite E/I effect in ASD has also been shown previously for the E/I-regulating drug, riluzole, measured by magnetic resonance spectroscopy (5). Importantly, our finding of an increase in *f*E/I through bumetanide in ASD is consistent with the open-label trial that found an increase in glutamate-to-GABA magnetic resonance spectroscopy concentrations in sensory cortices after 3 months of bumetanide treatment (33)—a shift toward a larger ratio between excitatory and inhibitory neurotransmission increases the power and *f*E/I also in the computational model used to develop the measure of E/I (53,54). Nonetheless, the direction of effects is counterintuitive when bumetanide is expected to reinstate hyperpolarizing GABA activity. Additional experiments are needed to gain understanding of the bumetanide effects on EEG, but we speculate that our network-level measure of E/I is sensitive to compensatory mechanisms, which might also be affected after 3 months of bumetanide treatment and may explain the seemingly paradoxical increase in network-level E/I. A homeostatic view has been postulated to gain understanding on how activity propagates in cortical circuits after E/I disruptions and how they may predict contradictory findings in ASD (13). In this scenario, we hypothesize from our findings that depolarizing GABA activity in neurodevelopmental disorders is balanced by a reduction in excitation. A bumetanide-induced shift in GABA polarity from depolarizing to hyperpolarizing effects may reduce the need for the compensatory excitatory downregulation and hence manifest as *f*E/I elevation in EEG signals. To test these ideas further, we plan follow-up EEG studies comparing immediate and sustained effects of treatment with bumetanide. Several other existing off-label drugs with a variety of GABAergic or glutamatergic actions have been tested in ASD using well-powered placebo-controlled trial designs (6,55–57). Most of these trials did not meet their primary end points, but most studies did find effects on secondary end points or subscales. Our findings encourage us to test these observations further and incorporate functional measures such as the EEG measures presented here with the collective aim to gain understanding on how they influence complex homeostatic E/I balance regulations and develop more stratified application strategies that acknowledge the physiological heterogeneity of ASD.

We did not find significant linear associations between EEG and outcome measures at the group level. We conducted subsequent correlation analyses testing different

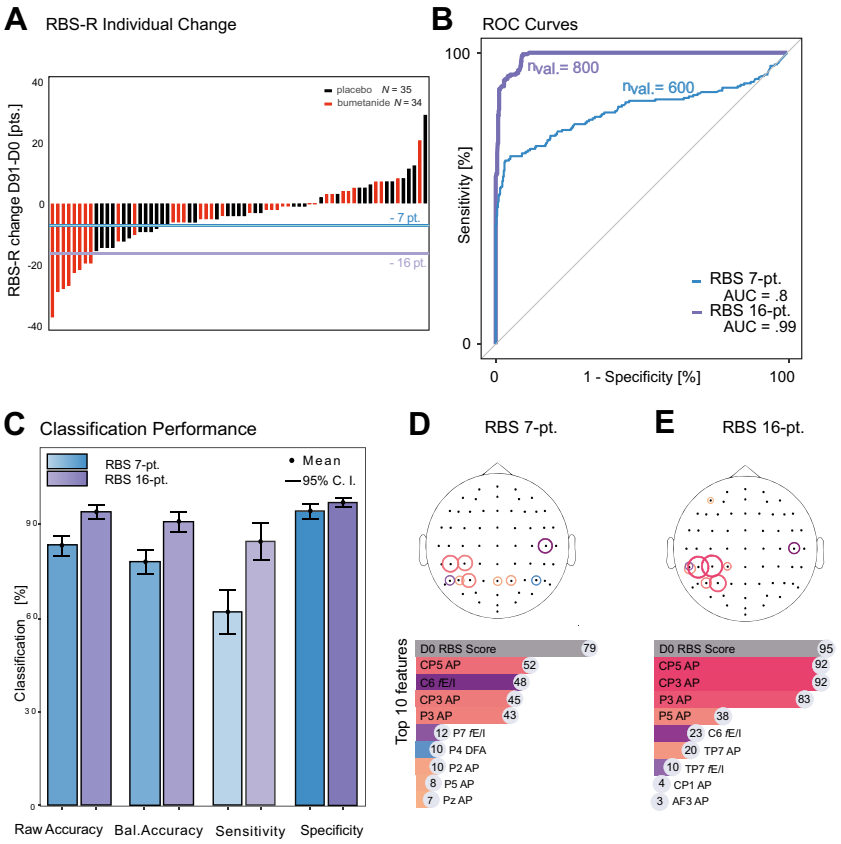

Figure 6. Machine learning shows best delineation between clinical improvement levels when predicting improvement in repetitive behavior. **(A)** Distribution of the individual change in Repetitive Behavior Scale-Revised (RBS-R) (D91−D0) in relation to treatment thresholds used for machine learning analysis (RBS 7-point blue line and RBS 16-point purple line). The data presented are only for individuals with pretreatment electroencephalography measures and clinical outcome scores available (bumetanide n = 34, placebo n = 35). **(B)** Receiver operating characteristic (ROC) curves to illustrate the diagnostic ability of the binary classifiers for the different improvement thresholds across the RBS-R outcome scales. This ability is expressed by the relationship between true (sensitivity) and false-positive rates, as depicted by the ROC curves. The curve for the perfect model that correctly classifies 100% below and above threshold improvers contains the point (0, 1), while a random estimate curve is closer to the nondiscrimination line (gray). An area under the curve (AUC) closer to 1 indicates a classifier having both high sensitivity and specificity. The best performance is indicated for 16-point RBS-R improvement, followed by a 7-point reduction. **(C)** Classification performance of RBS-R 7-point and RBS-R 16-point treatment thresholds. As per out-of-sample validation, the classifiers predicted 7-point and 16-point improvement on RBS-R with an average sensitivity of 63% and 86%, and 96% and 98.8% average specificity for each threshold, respectively, which corresponded to 79.5% and 92.4% average balanced accuracy (mean between specificity and sensitivity), respectively. **(D, E)** The 10 most frequently selected electrodes and electroencephalography measures in iterations exceeding 70% accuracy on validation partitions are shown for the two outcome thresholds. The baseline RBS-R score was most frequently selected as an important feature to inform RBS-R improvement, followed by absolute power in centroparietal channels (CP5 and CP3) and functional excitation-inhibition ratio (*f*E/I) in central channels (**C6**) for a medium RBS-R improvement (RBS-R 7-point) **(D)**, and absolute power in centroparietal channels (P3, CP5, CP3 and P5) for the high RBS-R improvement threshold (RBS-R 16-point) **(E)**. Bal., balanced; C. I., confidence interval; D0, day 0 baseline recording; D91, day 91 of treatment; DFA, detrended fluctuation analysis.

responsiveness thresholds under the hypothesis that participants with stronger improvement, and putatively less mixed with placebo-effects, might represent more true responsive subjects, i.e., where treatment effects are more likely related to the mechanism of action. The correlations between EEG and outcome measures observed in patients above the medium improvement threshold in repetitive behavior (RBS-R) may support this hypothesis and indicate utility of EEG for stratification of individuals likely to benefit from treatment. However, these subsample correlations need to be regarded as preliminary, requiring further validation as they lack power for generalization.

Through the machine learning analysis, we shifted from subgroup delineation to individualized predictions based on unique EEG and clinical values for each patient. The machine learning results indicated that baseline EEG measures can be used to predict improvement on the RBS-R scale in the bumetanide group with high accuracy, under both cross-validation and out-of-sample scenarios. The highest sensitivity (86%) was obtained when predicting a 16-point improvement on RBS-R, which suggests that pretreatment EEG measures and pretreatment RBS-R scores are more instrumental in identifying a high rather than a medium clinical improvement. SRS-2 predictions failed, which may be consistent with the fact that no superior treatment effect was found on this measure. We discussed in the first report of the BAMBI trial that repetitive behavior changes may be more readily observed after 3 months treatment than social behavioral change, which may be a more complex phenotype requiring longer treatment duration or additional behavioral therapy (58). Indeed, we found that RBS-R baseline score was selected most frequently in the predictions of both medium and high improvement thresholds. The results indicate that baseline RBS-R severity together with the most frequently selected absolute alpha power and *f*E/I in the parietal and central-parietal regions are most informative in predicting clinical improvement. The parietal cortex is relevant to ASD as it is a key area for integration of multiple stimuli (59) and considered part of the social brain network, with particular functions related to social cognition (60–63). Furthermore, the parietal area has been associated with functional E/I disturbances in ASD through a variety of imaging techniques (15,64). However, further prospective selected trials are needed to corroborate these feature combinations as potential ASD biotypes amenable to improvement through bumetanide treatment. Together, the correlations between the EEG and

clinical changes and the successful prediction of clinical improvement indicate clinical importance of the neurophysiological effect induced by bumetanide.

It is possible that bumetanide EEG effects are associated with improvement in symptoms intuitively related to network excitability, such as lack of energy, affect problems, or sleeping difficulty, which are not covered by the SRS-2 or RBS-R scales. Evaluation of individual, patient-relevant symptoms (rather than summed severity scores) may be valuable in future research. We restricted the current analysis to a selected set of EEG measures in the alpha frequency band that we previously found sensitive to the ratio of excitation and inhibition in computational models of neuronal networks (16,38). Expanding the analysis to other measures (17) and frequency bands can be considered for future studies. For the present study, however, this would have resulted in an excessive number of features relative to the sample size available for machine learning. The modest sample size coupled with a high dimensionality of the dataset may also have resulted in overfitting, albeit this was mitigated by out-of-sample validation. The validation in this study was conducted in such a manner that the optimistic bias resulting from a limited sample size was minimized. In addition, we reduced high dimensionality by selecting only the most informative features for prediction during feature selection. Because of the distribution of treatment responses in the sample, the high clinical improvement class is less likely to be identified correctly. This was reflected by sensitivity being generally lower than the specificity.

Conclusions

Quantitative analysis of alpha band resting-state EEG shows that bumetanide has neurophysiological effects in children with ASD. The out-of-sample treatment response predictions support the applicability of machine learning classification to future patient cohorts and encourage further development of EEG-assisted treatment decision-support systems.

ACKNOWLEDGMENTS AND DISCLOSURES

This work was supported by the Netherlands Organization for Scientific Research (NWO) Physical Sciences (Grant No. 612.001.123 [to KL-H]), Netherlands Organization for Scientific Research (NWO) Social Sciences (Grant No. 406-15-256 [to A-EA and KL-H]), ZonMW Rational Pharmacotherapy Program, GGG project (Grant No. 836041015 [to HB and JJS]), and EU H2020 "Human Brain Project" (Grant No. 604102 [to HDM]).

Neither the funders of the study nor Neurochlore, who provided the study medication, had a role in study design, data collection, data analysis, data interpretation, or writing of the report.

Conceptualization: HB and KL-H; methodology: ELJ-M, JJS, GC, GJvdW, MJCE, KL-H, HB; investigation: ELJ-M, JJS, GC; visualization: ELJ-M, JJS, GC, SS, A-EA, SJH; acquisition, analysis, or interpretation of data: all authors; funding acquisition: KL-H, HB; administrative, technical, or material support: SS, A-EA, RH, SJH, BO; supervision: HDM, KL-H, HB; writing - original draft: ELJ-M, JJS, GC, KL-H, HB; and writing - reviewing and editing: all authors.

We thank Simon-Shlomo Poil for contributions to the Neurophysiological Biomarker Toolbox. We thank Neurochlore for providing the study medication.

Due to privacy regulations of human subjects, we cannot provide the electroencephalography files of the subjects included in our study. However, we provide the individual demographics and the mean of electroencephalography measures in Tables S1 and S2. Analysis scripts to reproduce the figures and statistics will be made available on figshare (https://figshare.com/). The code for the *f*E/I algorithm is publicly available at https://github.com/rhardstone/fEI.

KL-H and Simon-Shlomo Poil are shareholders of NBT Analytics BV, which provides EEG analysis services for clinical trials. HB, KL-H, and Simon-Shlomo Poil are shareholders of Aspect Neuroprofiles BV, which develops physiology-informed prognostic measures for neurodevelopmental disorders. RH and KL-H have filed the patent claim (PCT/NL2019/050167) "Method of determining brain activity"; with priority date March 16, 2018. All other authors report no biomedical financial interests or potential conflicts of interest.

EudraCT: EU Clinical Trials Register; https://www.clinicaltrialsregister.eu/ctr-search/trial/2014-001560-35/NL; 2014-001560-35.

ARTICLE INFORMATION

From the Department of Integrative Neurophysiology (ELJ-M, A-EA, SS, SJH, HDM, KL-H), Center for Neurogenomics and Cognitive Research, Neuroscience, VU University Amsterdam, Amsterdam; NBT Analytics BV (ELJ-M, SS), Amsterdam; Child and Adolescent Psychiatry and Psychosocial Care (ELJ-M, GC, CG, HB), Emma Children's Hospital, Amsterdam UMC, Vrije Universiteit Amsterdam, Amsterdam; N=You Neurodevelopmental Precision Center (GC, CG, HB), Amsterdam Neuroscience, Amsterdam Reproduction and Development, Amsterdam UMC, Amsterdam; Levvel (HB), Center for Child and Adolescent Psychiatry, Amsterdam; Department of Psychiatry (JJS, BO, DMvA, CG, MJCE, HB), UMC Utrecht Brain Center, University Medical Centre Utrecht, Utrecht; Department of Biostatistics & Research Support (MJCE), Julius Center for Health Sciences and Primary Care, University Medical Centre Utrecht; and Department of Health Evidence (GC, GJvdW), Radboud University Medical Center, Nijmegen, The Netherlands; and Neuroscience Institute (RH), New York University School of Medicine, New York, New York.

ELJ-M, JJS, and GC contributed equally to this work.

KL-H and HB contributed equally to this work.

Address correspondence to Hilgo Bruining, M.D., Ph.D., at h.bruining@amsterdamumc.nl.

Received Jul 1, 2021; revised Jul 31, 2021; accepted Aug 26, 2021.

Supplementary material cited in this article is available online at https://doi.org/10.1016/j.bpsc.2021.08.009.

REFERENCES

1. Thapar A, Cooper M, Rutter M (2017): Neurodevelopmental disorders. Lancet Psychiatry 4:339–346.
2. Lord C, Elsabbagh M, Baird G, Veenstra-Vanderweele J (2018): Autism spectrum disorder. Lancet 392:508–520.
3. McPheeters ML, Warren Z, Sathe N, Bruzek JL, Krishnaswami S, Jerome RN, Veenstra-Vanderweele J (2011): A systematic review of medical treatments for children with autism spectrum disorders. Pediatrics 127:e1312–e1321.
4. de la Torre-Ubieta L, Won H, Stein JL, Geschwind DH (2016): Advancing the understanding of autism disease mechanisms through genetics. Nat Med 22:345–361.
5. Ajram LA, Horder J, Mendez MA, Galanopoulos A, Brennan LP, Wichers RH, *et al.* (2017): Shifting brain inhibitory balance and connectivity of the prefrontal cortex of adults with autism spectrum disorder. Transl Psychiatry 7:e1137.
6. Veenstra-VanderWeele J, Cook EH, King BH, Zarevics P, Cherubini M, Walton-Bowen K, *et al.* (2017): Arbaclofen in children and adolescents with autism spectrum disorder: A randomized, controlled, phase 2 trial. Neuropsychopharmacology 42:1390–1398.
7. Anagnostou E (2018): Clinical trials in autism spectrum disorder: Evidence, challenges and future directions. Curr Opin Neurol 31:119–125.
8. Charman T, Loth E, Tillmann J, Crawley D, Wooldridge C, Goyard D, *et al.* (2017): The EU-AIMS Longitudinal European Autism Project (LEAP): Clinical characterisation. Mol Autism 8:27.
9. Wang J, Barstein J, Ethridge LE, Mosconi MW, Takarae Y, Sweeney JA (2013): Resting state EEG abnormalities in autism spectrum disorders. J Neurodev Disord 5:24.

10. Jeste SS, Frohlich J, Loo SK (2015): Electrophysiological biomarkers of diagnosis and outcome in neurodevelopmental disorders. Curr Opin Neurol 28:110–116.
11. Heunis TM, Aldrich C, de Vries PJ (2016): Recent advances in resting-state electroencephalography biomarkers for autism spectrum disorder-A review of methodological and clinical challenges. Pediatr Neurol 61:28–37.
12. Dickinson A, Jones M, Milne E (2016): Measuring neural excitation and inhibition in autism: Different approaches, different findings and different interpretations. Brain Res 1648:277–289.
13. Nelson SB, Valakh V (2015): Excitatory/inhibitory balance and circuit homeostasis in autism spectrum disorders. Neuron 87:684–698.
14. Rubenstein JL, Merzenich MM (2003): Model of autism: Increased ratio of excitation/inhibition in key neural systems. Genes Brain Behav 2:255–267.
15. Uzunova G, Pallanti S, Hollander E (2016): Excitatory/inhibitory imbalance in autism spectrum disorders: Implications for interventions and therapeutics. World J Biol Psychiatry 17:174–186.
16. Bruining H, Hardstone R, Juarez-Martinez EL, Sprengers J, Avramiea AE, Simpraga S, *et al.* (2020): Measurement of excitation-inhibition ratio in autism spectrum disorder using critical brain dynamics. Sci Rep 10:9195.
17. Donoghue T, Haller M, Peterson EJ, Varma P, Sebastian P, Gao R, *et al.* (2020): Parameterizing neural power spectra into periodic and aperiodic components. Nat Neurosci 23:1655–1665.
18. Murias M, Major S, Compton S, Buttinger J, Sun JM, Kurtzberg J, Dawson G (2018): Electrophysiological biomarkers predict clinical improvement in an open-label trial assessing efficacy of autologous umbilical cord blood for treatment of autism. Stem Cells Transl Med 7:783–791.
19. Roberts TPL, Bloy L, Blaskey L, Kuschner E, Gaetz L, Anwar A, *et al.* (2019): A MEG study of acute Arbaclofen (STX-209) administration. Front Integr Neurosci 13:69.
20. Sinclair D, Featherstone R, Naschek M, Nam J, Du A, Wright S, *et al.* (2017): GABA-B agonist baclofen normalizes auditory-evoked neural oscillations and behavioral deficits in the Fmr1 knockout mouse model of fragile X syndrome. eNeuro 4: ENEURO.0380-16.2017.
21. Knociková JA, Vejmola Č., Klovrza O, Petrásek T (2020): Nonlinear measure of EEG complexity in the Eker Rat model of autism disorder: A pilot study. In: In: ICoMS 2020: Proceedings of the 2020 3rd International Conference on Mathematics and Statistics. New York: Association for Computing Machinery, 49–53.
22. van Andel DM, Sprengers JJ, Oranje B, Scheepers FE, Jansen FE, Bruining H (2020): Effects of bumetanide on neurodevelopmental impairments in patients with tuberous sclerosis complex: An open-label pilot study. Mol Autism 11:30.
23. Raz N, Pritchard WS, August GJ (1987): Effects of fenfluramine on EEG and brainstem average evoked response in infantile autism. Preliminary investigation. Neuropsychobiology 18:105–109.
24. Kouijzer ME, van Schie HT, Gerrits BJ, Buitelaar JK, de Moor JM (2013): Is EEG-biofeedback an effective treatment in autism spectrum disorders? A randomized controlled trial. Appl Psychophysiol Biofeedback 38:17–28.
25. Dawson G, Jones EJ, Merkle K, Venema K, Lowy R, Faja S, *et al.* (2012): Early behavioral intervention is associated with normalized brain activity in young children with autism. J Am Acad Child Adolesc Psychiatry 51:1150–1159.
26. Sokhadze EM, Baruth JM, Sears L, Sokhadze GE, El-Baz AS, Casanova MF (2012): Prefrontal neuromodulation using rTMS improves error monitoring and correction function in autism. Appl Psychophysiol Biofeedback 37:91–102.
27. Zhdanov A, Atluri S, Wong W, Vaghei Y, Daskalakis ZJ, Blumberger DM, *et al.* (2020): Use of machine learning for predicting escitalopram treatment outcome from electroencephalography recordings in adult patients with depression. JAMA Netw Open 3: e1918377.
28. Wu W, Zhang Y, Jiang J, Lucas MV, Fonzo GA, Rolle CE, *et al.* (2020): An electroencephalographic signature predicts antidepressant response in major depression. Nat Biotechnol 38:439–447.
29. Rajpurkar P, Yang J, Dass N, Vale V, Keller AS, Irvin J, *et al.* (2020): Evaluation of a machine learning model based on pretreatment symptoms and electroencephalographic features to predict outcomes of antidepressant treatment in adults with depression: A prespecified secondary analysis of a randomized clinical trial [published correction appears in JAMA Netw Open 2020;3:e2016001]. JAMA Netw Open 3: e206653.
30. Ben-Ari Y (2002): Excitatory actions of GABA during development: The nature of the nurture. Nat Rev Neurosci 3:728–739.
31. Ben-Ari Y, Khalilov I, Kahle KT, Cherubini E (2012): The GABA excitatory/inhibitory shift in brain maturation and neurological disorders. Neuroscientist 18:467–486.
32. Kharod SC, Kang SK, Kadam SD (2019): Off-label use of bumetanide for brain disorders: An overview. Front Neurosci 13:310.
33. Zhang L, Huang CC, Dai Y, Luo Q, Ji Y, Wang K, *et al.* (2020): Symptom improvement in children with autism spectrum disorder following bumetanide administration is associated with decreased GABA/glutamate ratios [published correction appears in Transl Psychiatry 2020;10:63]. Transl Psychiatry 10:9.
34. Lemonnier E, Villeneuve N, Sonie S, Serret S, Rosier A, Roue M, *et al.* (2017): Effects of bumetanide on neurobehavioral function in children and adolescents with autism spectrum disorders. Transl Psychiatry 7:e1124.
35. Lemonnier E, Degrez C, Phelep M, Tyzio R, Josse F, Grandgeorge M, *et al.* (2012): A randomised controlled trial of bumetanide in the treatment of autism in children. Transl Psychiatry 2:e202.
36. Sprengers JJ, van Andel DM, Zuithoff NPA, Keijzer-Veen MG, Schulp AJA, Scheepers FE, *et al.* (2021): Bumetanide for core symptoms of autism spectrum disorder (BAMBI): A single center, double-blinded, participant-randomized, placebo-controlled, phase-2 superiority trial. J Am Acad Child Adolesc Psychiatry 60:865–876.
37. Hardstone R, Poil SS, Schiavone G, Jansen R, Nikulin VV, Mansvelder HD, Linkenkaer-Hansen K (2012): Detrended fluctuation analysis: A scale-free view on neuronal oscillations. Front Physiol 3:450.
38. Poil SS, Hardstone R, Mansvelder HD, Linkenkaer-Hansen K (2012): Critical-state dynamics of avalanches and oscillations jointly emerge from balanced excitation/inhibition in neuronal networks. J Neurosci 32:9817–9823.
39. Peng CK, Havlin S, Stanley HE, Goldberger AL (1995): Quantification of scaling exponents and crossover phenomena in nonstationary heartbeat time series. Chaos 5:82–87.
40. Kahan BC, Cro S, Doré CJ, Bratton DJ, Rehal S, Maskell NA, *et al.* (2014): Reducing bias in open-label trials where blinded outcome assessment is not feasible: Strategies from two randomised trials. Trials 15:456.
41. Thompson DD, Lingsma HF, Whiteley WN, Murray GD, Steyerberg EW (2015): Covariate adjustment had similar benefits in small and large randomized controlled trials. J Clin Epidemiol 68:1068–1075.
42. Team R (2020): RStudio: Integrated Development for R. Boston: RStudio.
43. R Core Team (2020): R: A Language and Environment for Statistical Computing. Vienna: R Foundation for Statistical Computing.
44. Poldrack RA, Huckins G, Varoquaux G (2020): Establishment of best practices for evidence for prediction: A review. JAMA Psychiatry 77:534–540.
45. Wright MN, Ziegler A (2017): ranger: A fast implementation of random forests for high dimensional data in C++ and R. J Stat Softw 77:1–17.
46. Hadjikhani N, Åsberg Johnels J, Lassalle A, Zürcher NR, Hippolyte L, Gillberg C, *et al.* (2018): Bumetanide for autism: More eye contact, less amygdala activation. Sci Rep 8:3602.
47. Vlaskamp C, Poil SS, Jansen F, Linkenkaer-Hansen K, Durston S, Oranje B, Bruining H (2017): Bumetanide as a candidate treatment for behavioral problems in tuberous sclerosis complex. Front Neurol 8:469.
48. Bruining H, Passtoors L, Goriounova N, Jansen F, Hakvoort B, de Jonge M, Poil SS (2015): Paradoxical benzodiazepine response: A

rationale for bumetanide in neurodevelopmental disorders? Pediatrics 136:e539–e543.
49. Puskarjov M, Kahle KT, Ruusuvuori E, Kaila K (2014): Pharmacotherapeutic targeting of cation-chloride cotransporters in neonatal seizures. Epilepsia 55:806–818.
50. Ben-Ari Y (2017): NKCC1 chloride importer antagonists attenuate many neurological and psychiatric disorders. Trends Neurosci 40:536–554.
51. Lozano-Soldevilla D (2018): On the physiological modulation and potential mechanisms underlying parieto-occipital alpha oscillations. Front Comput Neurosci 12:23.
52. Lozano-Soldevilla D, ter Huurne N, Cools R, Jensen O (2014): GABAergic modulation of visual gamma and alpha oscillations and its consequences for working memory performance. Curr Biol 24:2878–2887.
53. Pfeffer T, Avramiea AE, Nolte G, Engel AK, Linkenkaer-Hansen K, Donner TH (2018): Catecholamines alter the intrinsic variability of cortical population activity and perception. PLoS Biol 16: e2003453.
54. Avramiea AE, Hardstone R, Lueckmann JM, Bím J, Mansvelder HD, Linkenkaer-Hansen K (2020): Pre-stimulus phase and amplitude regulation of phase-locked responses are maximized in the critical state. Elife 9:e53016.
55. Hardan AY, Hendren RL, Aman MG, Robb A, Melmed RD, Andersen KA, *et al.* (2019): Efficacy and safety of memantine in children with autism spectrum disorder: Results from three phase 2 multicenter studies. Autism 23:2096–2111.
56. Wink LK, Adams R, Horn PS, Tessier CR, Bantel AP, Hong M, *et al.* (2018): A randomized placebo-controlled cross-over pilot study of riluzole for drug-refractory irritability in autism spectrum disorder. J Autism Dev Disord 48:3051–3060.
57. Minshawi NF, Wink LK, Shaffer R, Plawecki MH, Posey DJ, Liu H, *et al.* (2016): A randomized, placebo-controlled trial of D-cycloserine for the enhancement of social skills training in autism spectrum disorders. Mol Autism 7:2.
58. Anagnostou E, Jones N, Huerta M, Halladay AK, Wang P, Scahill L, *et al.* (2015): Measuring social communication behaviors as a treatment endpoint in individuals with autism spectrum disorder. Autism 19:622–636.
59. Teixeira S, Machado S, Velasques B, Sanfim A, Minc D, Peressutti C, *et al.* (2014): Integrative parietal cortex processes: Neurological and psychiatric aspects. J Neurol Sci 338:12–22.
60. Saxe R, Kanwisher N (2003): People thinking about thinking people. The role of the temporo-parietal junction in "theory of mind". Neuroimage 19:1835–1842.
61. Sperdin HF, Coito A, Kojovic N, Rihs TA, Jan RK, Franchini M, *et al.* (2018): Early alterations of social brain networks in young children with autism. Elife 7:e31670.
62. Molapour T, Hagan CC, Silston B, Wu H, Ramstead M, Friston K, Mobbs D (2021): Seven computations of the social brain. Soc Cogn Affect Neurosci 16:745–760.
63. Fujii N, Hihara S, Iriki A (2008): Social cognition in premotor and parietal cortex. Soc Neurosci 3:250–260.
64. Holiga Ś, Hipp JF, Chatham CH, Garces P, Spooren W, D'Ardhuy XL, *et al.* (2019): Patients with autism spectrum disorders display reproducible functional connectivity alterations. Sci Transl Med 11: eaat9223.